

**This is the preprint of the contribution published as:**

**Toepel, J., Karande, R., Bühler, B., Bühler, K., Schmid, A. (2023):**

Photosynthesis driven continuous hydrogen production by diazotrophic cyanobacteria in high cell density capillary photobiofilm reactors

*Bioresour. Technol.* **373** , art. 128703

**The publisher's version is available at:**

<http://dx.doi.org/10.1016/j.biortech.2023.128703>

1  
  
2  
  
3  
  
4  
  
5  
  
6  
  
7  
  
8  
  
9  
  
10  
  
11  
  
12  
  
13  
  
14  
  
15  
  
16  
  
17  
  
18  
  
19  
  
20

Photosynthesis driven continuous hydrogen production by  
diazotrophic cyanobacteria in high cell density capillary photobiofilm  
reactors

Journal: Bioresource Technology

Authors: Jörg Toepel, Rohan Karande, Bruno Bühler, Katja Bühler and Andreas  
Schmid

Department Solar Materials; Helmholtz Center for Environmental Research Leipzig

Permoser Strasse 15

04315 Leipzig

Germany

Corresponding author: Jörg Toepel

[Joerg.toepel@ufz.de](mailto:Joerg.toepel@ufz.de)

21  
  
22  
  
23  
  
24  
  
25  
  
26  
  
27  
  
28  
  
29  
  
30  
  
31  
  
32  
  
33  
  
34  
  
35  
  
36  
  
37  
  
38  
  
39  
  
40  
  
41

Abstract

Hydrogen (H<sub>2</sub>) is a promising fuel in the context of climate neutral energy carriers and photosynthesis-driven H<sub>2</sub>-production is an interesting option relying mainly on sunlight and water as resources. However, this approach depends on suitable biocatalysts and innovative photobioreactor designs to maximize cell performance and H<sub>2</sub> titers. Cyanobacteria were used as biocatalysts in capillary biofilm photobioreactors (CBRs). We show that biofilm formation/stability depend on light and CO<sub>2</sub> availability. H<sub>2</sub> production rates correlate with these parameters but differ between *Anabaena* and *Nostoc*. We demonstrate that high light and corresponding O<sub>2</sub> levels influence biofilm stability in CBR. By adjusting these parameters, biofilm formation/stability could be enhanced, and H<sub>2</sub> formation was stable for weeks. Final biocatalyst titers reached up to 100 g l<sup>-1</sup> for *N. punctiforme* ATCC29133 NHM5 and *Anabaena* sp. PCC7120 AMC 414. H<sub>2</sub> production rates were up to 300 μmol H<sub>2</sub> l<sup>-1</sup> h<sup>-1</sup> and 3 μmol H<sub>2</sub> g<sub>cdw</sub><sup>-1</sup> h<sup>-1</sup> in biofilms.

Keywords:

Photosynthesis driven hydrogen production

Capillary biofilm photobioreactors

Cyanobacteria

## Introduction

Molecular hydrogen ( $H_2$ ) is an important energy carrier for a future, non-fossil energy landscape. Different concepts for sustainable  $H_2$  production have been described (Bühler et al., 2021). The main focus is currently on water electrolysis driven by renewable energy derived, e.g., from wind or sun. However, electrolysis depends on noble metal catalysts with limited availability. Photosynthesis-driven  $H_2$  production is potentially carbon-neutral, relying on sunlight, abundant salts, and water as major resources for biocatalyst operation (Khetkorn et al., 2017; Tiwari & Pandey, 2012). Since several decades, researchers work on wiring  $H_2$  production to the photosynthetic apparatus of cyanobacteria or green algae performing oxygenic photosynthesis (Krishnan et al., 2018; Martin & Frymier, 2017). Nitrogenases and hydrogenases are the most promising enzymes to make use of photosynthesis-derived reduction equivalents for  $H_2$  formation (Bothe, 2016). However, the pronounced  $O_2$  sensitivity of most of these enzymes hamper biotechnological applications, especially when applied in phototrophs performing oxygenic photosynthesis. Current approaches for  $H_2$  production involve either the (temporary) establishment of anaerobic conditions or the use of diazotrophic cyanobacteria forming heterocysts as anaerobic reaction compartments for operating  $O_2$ -sensitive enzymes. Yet, both approaches suffer from an indirect and thus inefficient coupling of  $H_2$  formation to photosynthesis. The advantage of diazotrophic cyanobacteria is their independence of cost-intensive nitrogen source feeding. This may enable low production costs and could also provide valuable biomass with high N content for other applications like animal feed or fertilizers (Pathak et al., 2018).

Conventional photobioreactor systems are often limited in productivity by low biomass concentrations due to illumination efficiency, gas mass transfer (especially

low carbon availability), product removal, nutrient supply, and relatively high operation costs (Posten, 2009). These features typically result in slow cell growth, low cell densities, and short process times with narrow production windows and low productivities (Fernandes et al., 2015; Fu et al., 2019; Hariskos & Posten, 2014; Johnson et al., 2018; Kirnev et al., 2020). New cultivation concepts to achieve high, stable, and potentially scalable productivities for the phototrophic production of biomass, chemicals, and fuels involve, e.g., cell retention / immobilization in membrane photobioreactors or biofilm photobioreactors (Bähr et al., 2016; ; Li et al., 2019; Podola et al., 2017; Schultze et al., 2015). In addition, several studies demonstrated that artificial or natural biofilms enable enhanced and prolonged biomass production and product formation (Schultze et al., 2015; Zhang et al., 2017). However, artificial cell immobilization is limited by the stability of encapsulated cells (Homburg et al., 2019; Vorndran & Lindberg, 2016). Capillary photobiofilm reactors, CBRs, based on natural biofilm formation, were reported as a promising solution, as previously shown for photosynthesis-driven oxyfunctionalization of cyclohexane to cyclohexanol (Hoschek et al., 2019). The capillary biofilm reactor concept set a benchmark regarding achievable biomass concentration (up to 58 g<sub>cdw</sub> L<sup>-1</sup>) and productivity for selective C-H hydroxylation (up to 3.76 g cyclohexanol m<sup>-2</sup> day<sup>-1</sup>) applying recombinant *Synechocystis* sp. PCC 6803 cells as biocatalysts. Recently, the application was extended to other cyanobacteria, demonstrating the potential and importance of a photo- and heterotrophic co-cultivation and the possibility to use diazotrophic cyanobacteria with nitrogen free media (Bozan et al., 2022) for the production of H<sub>2</sub>. Several studies showed that additional factors define H<sub>2</sub> production, namely biofilm thickness and biofilm structure (Liao et al., 2015), which in turn are influenced by surface properties of the capillaries and can be tuned by applying special coatings (Li et al., 2017). Capillary biofilm bioreactors have also been applied

to concepts based on dark fermentation (Renaudie et al., 2021) and combined approaches of dark fermentation and photo-  $H_2$  production (Cheng et al., 2022).

Here, the suitability of CBRs for continuous  $H_2$  production with diazotrophic cyanobacteria was investigated. Up to date, the highest productivities for  $H_2$  formation in light and thus in the presence of photosynthetic water oxidation are reported for diazotrophic filamentous cyanobacteria. These microbes produce  $H_2$  as a side product during  $N_2$  fixation in heterocysts. In the natural system, the energy in the produced  $H_2$  is metabolically recycled via an uptake hydrogenase. In the two model strains employed in this study, the respective uptake hydrogenases have been deleted, although *Anabaena* sp. PCC 7120 still contains a bidirectional hydrogenase. However, it was shown that  $H_2$  production is typically not impaired by this enzyme (Masukawa et al., 2002).

The productivity of the CBR reactor regarding  $H_2$  formation was quantified. Importantly, the impact of parameters like light intensity and  $O_2$  concentration on biofilm development and stability as well as  $H_2$  productivity was investigated. Two filamentous, diazotrophic cyanobacteria, *Nostoc punctiforme* ATCC 29133 NHM5 and *Anabaena* sp. PCC 7120 AMC 414 lacking  $H_2$  uptake hydrogenases showed high  $H_2$  production rates in continuous capillary photobioreactors. This study highlights future strain and reactor engineering targets paving the way for efficient photosynthesis-driven  $H_2$  production using biocatalysts based on biofilm forming cyanobacteria.

## Material and Methods

### Strains & shake flask cultivation

The two uptake hydrogenase-deficient filamentous diazotrophic cyanobacterial strains, *Nostoc punctiforme* ATCC 29133 NHM5 ( $\Delta hupL$ ), hereafter called NHM5, and

*Anabaena* sp. PCC 7120 AMC 414 ( $\Delta$ xisC, recombinase), hereafter named AMC 414, and the corresponding wild type strains were investigated (see the list of strains used in this study, Table 1). All strains were cultivated in BG-11 medium (buffered 10 mM HEPES; pH 7.2)(with nitrate) (Lindberg et al., 2002) at 30°C under continuous white light (25  $\mu$ mol photons m<sup>-2</sup> s<sup>-1</sup>) in Erlenmeyer flasks in a multitron shaker (Infors, Bottmingen, Switzerland) prior to inoculation in CBRs, as described previously (Figure 1) (Heuschkel et al., 2019b; Hoschek et al., 2019). *Pseudomonas taiwanensis* VLB 120 was cultivated as described previously and mixed in a defined ratio prior to biofilm inoculation and cultivation (Bozan et al., 2022).

#### Capillary biofilm reactor operation

Polystyrene capillaries (25 cm length, 3 mm inner diameter, 1.76 ml) were used as bioreactor units. The capillary diameter was intentionally selected to obtain a high surface area to volume ratio (1333 m<sup>2</sup> m<sup>-3</sup>) and low light penetration depth. In addition, the described aqueous-air slug flow enables Taylor flow conditions beneficial for maximizing the mass transfer of heat, nutrients and gaseous compounds. As shown previously, (Hoschek et al, 2019), these conditions stabilize biofilm thickness, prevent congestion and prevent limiting mass transfer of nutrients and gases. Polystyrene was selected as material, to minimize diffusion-related H<sub>2</sub> loss. Defined mixtures of *P. taiwanensis* VLB 120 and the cyanobacterial strains were inoculated as described for initial biofilm formation (Hoschek et al., 2019). Operating the CBRs in a segmented flow regime (Figure 1), BG-11 medium and air were applied at an equal flow rate of 52  $\mu$ l min<sup>-1</sup> using a peristaltic pump (Ismatec, Wertheim, Germany) under continuous illumination at room temperature (air-conditioned to 25°C). H<sub>2</sub> production was induced by switching to diazotrophic conditions (applying nitrogen-free BG-11<sub>0</sub> medium). Keeping the gas flow constant, the gas composition was varied, reducing the O<sub>2</sub>

concentration by replacing air with argon or nitrogen via a gas-tight balloon filled with the respective gas and connected to the airflow line. The gas composition in the CBRs was measured as described below. The biofilm dry weight was determined at the end of the experiments as described previously (Hoschek et al., 2019). Light was applied with a LED light system (Cell Deg, Berlin, Germany) at intensities ranging from 25 to 150  $\mu\text{mol photons m}^{-2} \text{ s}^{-1}$ . It is important to note that the LED provided blue (460 nm) and red light (660 and 680 nm), being photosynthetically more effective than white light. Sodium bicarbonate (Sigma-Aldrich) was added to the media (0-20 mM) as a carbon source.

## H<sub>2</sub> – quantification / analysis

Custom-made bubble traps were connected to the outlet of the cultivation unit for H<sub>2</sub> and O<sub>2</sub> quantification. The bubble trap system (1 ml total volume) was flushed with air after every sampling of the gas phase (5 ml). A gas-tight syringe (Hamilton, Reno, NV) was inserted into the bubble trap, and 100  $\mu\text{L}$  gas phase were withdrawn and manually injected into a gas chromatograph (Thermo scientific, Trace1310 equipped with a TG Bond MIsieve 5A column with 0.32 mm inner diameter and 0.20  $\mu\text{m}$  film thickness). The thermal conductivity detector and the oven were adjusted to 100 and 75°C, respectively. Gas concentrations were calculated based on calibration curves determined with defined gas mixtures. Volumetric and biomass specific H<sub>2</sub> production rates were calculated based on the percentage of H<sub>2</sub> in the gas phase, the flow rate, and the biomass in the capillaries.

H<sub>2</sub> production by all strains was additionally determined for cell suspensions in closed vials. Cells were cultivated in BG-11 medium as described above. H<sub>2</sub> production was induced by transferring the cells into BG-11<sub>0</sub> medium. To this end, cells harvested by centrifugation (4000g, room temperature) were washed twice with BG-11<sub>0</sub> medium



followed by resuspension in the same medium. Upon continued incubation in Erlenmeyer flasks, cell suspension samples (5 mL) were taken 24, 48, and 72 h after the transfer to BG-11<sub>0</sub> medium, transferred into sealed GC vials (Thermo Scientific), supplied with 10 mM sodium bicarbonate, and incubated for 24 h at 30°C under continuous light (50  $\mu\text{mol photons m}^{-2} \text{s}^{-1}$ ) to quantify H<sub>2</sub> production. H<sub>2</sub> formation rates were determined by GC analysis of the gas phase as described above.

## Results and discussion

### H<sub>2</sub> production in planktonic cultures

H<sub>2</sub> production of all strains (*Nostoc punctiforme* ATCC 29133 WT, *Nostoc punctiforme* ATCC 29133 NHM5, *Anabaena* sp. PCC 7120 WT, *Anabaena* sp. PCC 7120 AMC 414) was first tested in planktonic cultures. Cell suspensions in BG-11<sub>0</sub> (5 ml) were incubated in a multitron cultivation chamber (Infors) in closed 20 ml GC vials (Thermo Scientific) under illumination (25  $\mu\text{mol photons m}^{-2} \text{s}^{-1}$ ). H<sub>2</sub> formation rates were determined 24, 48, and 72 h after transition into nitrogen-free BG-11<sub>0</sub> medium. Samples taken at these time points were incubated in sealed vials, and H<sub>2</sub> accumulation was analyzed (see materials and methods section for details). For NHM5, high activities were measured after 24 h indicating heterocyst development, whereas this was found to take 48 h in the case of AMC 414. The hydrogenase-deficient strains showed 5 times higher biomass specific H<sub>2</sub> formation rates compared to the corresponding wild type (WT) strains. NHM5 showed the highest specific H<sub>2</sub> formation rate (15  $\mu\text{mol H}_2 \text{ g}_{\text{cdw}}^{-1} \text{ h}^{-1}$ , with an average rate of  $12 \pm 3.5 \mu\text{mol H}_2 \text{ g}_{\text{cdw}}^{-1} \text{ h}^{-1}$  rates measured for samples taken after 24, 48, and 72 h). For AMC 414, this highest rate was  $12 \mu\text{mol H}_2 \text{ g}_{\text{cdw}}^{-1} \text{ h}^{-1}$ , 48 h after nitrogen deprivation (average:  $8 \pm 4 \mu\text{mol H}_2 \text{ g}_{\text{cdw}}^{-1} \text{ h}^{-1}$ ). Assuming that Chl a accounts for 1% of the cell dry weight (Zavrel et al., 2019), these rates translate into 1.5 and 1.2  $\mu\text{mol H}_2 (\text{mg Chl a})^{-1} \text{ h}^{-1}$ , respectively.

## H<sub>2</sub> production in capillary biofilm photobioreactors

Biofilm development of *N. punctiforme* ATCC 29133, *Anabaena* sp. PCC 7120, and their respective hydrogenase-deficient mutants was analyzed in capillary biofilm photobioreactors (CBRs) as a first step towards biofilm-based H<sub>2</sub> production. Co-cultivation with *P. taiwanensis* VLB120 has been reported to promote biofilm formation with the cyanobacterial strains *Synechocystis* sp. PCC 6803 (Heuschkel et al., 2019b; Hoschek et al., 2019) and *Tolypotrix* sp. PCC 7712 (Bozan et al., 2022). Similarly, only very poor or no biofilm formation was detected for monoseptic CBR cultures of NHM5, AMC 414, and respective wildtype strains, whereas good biofilm growth was obtained upon co-cultivation with *P. taiwanensis* VLB120 (data not shown). Thereby, no addition of an organic carbon source was necessary. Uptake hydrogenase deletion strains and respective WT strains showed identical growth behaviors. Biofilm formation was slightly enhanced in terms of surface coverage upon nitrogen deprivation resulting in biomass concentrations of 8-10 g<sub>cdw</sub> l<sup>-1</sup>. The optimal initial cell ratio of cyanobacteria and heterotrophic partner was determined to be 1:1, enabling optimal biofilm formation and minimal biofilm detachment. It is important to note that the heterotrophic cells are mainly needed for initial biofilm formation. The final fraction of *Pseudomonas* cells in the biofilm is very low, especially, when no organic carbon and energy source is added (Heuschkel et al. 2019a, Bozan et al. 2022), like in the process reported here. Therefore, cyanobacterial cells are the main species in the biofilm in the final stadium. Neither *N. punctiforme* WT nor *Anabaena* WT produced H<sub>2</sub> during CBR cultivations, whereas the respective H<sub>2</sub> uptake-deficient strains in co-culture with *P. taiwanensis* VLB120 showed H<sub>2</sub> production. It is important to note that the determined biomass consists of both species in all biofilm experiments, whereas the heterotrophic cells were present in low amounts, see also Bozan et al. (2022). Average H<sub>2</sub> production rates amounted to 72 ± 22 (NHM5) and 150 ± 47 μmol H<sub>2</sub> l<sup>-1</sup> h<sup>-1</sup> (AMC 414) for 14 days

(Figure 2). However, the daily H<sub>2</sub> formation rates varied significantly, and biofilms remained patchy in terms of surface coverage (see supplemental material). Remarkably, these rates correspond to similar specific rates as measured for suspended cells, for which, however, H<sub>2</sub> formation rates may not have been constant in the analyzed 24 h time range.

The poor surface coverage in the first CBR experiments indicated that growth and H<sub>2</sub> production were limited. So, what parameters are basically determining growth, biofilm formation and the H<sub>2</sub> formation rate? After initial biofilm formation, sodium bicarbonate supply (10 mM) to the BG-11<sub>0</sub> medium was tested and indeed improved biofilm formation and H<sub>2</sub> production (Figure 3 (I)). Both uptake hydrogenase-deficient strains showed enhanced growth and surface coverage, which, however, was still lower than described for *Synechocystis* sp. PCC 6803 (Hoschek et al., 2019). H<sub>2</sub> formation rates with both strains increased in the beginning and were then stable for several days with 300 μmol H<sub>2</sub> l<sup>-1</sup> h<sup>-1</sup> for NHM5 and 75 μmol H<sub>2</sub> l<sup>-1</sup> h<sup>-1</sup> for AMC 414. NHM5 produced 4 times more H<sub>2</sub> compared to AMC 414 and to conditions without carbonate, whereas AMC 414 produced only half the amount of H<sub>2</sub> compared to conditions without carbonate. To test whether H<sub>2</sub> production is still limited by carbon availability, the sodium bicarbonate concentration was increased to 20 mM (Figure 3 (II)). However, biofilm stability with NHM5 was impaired and detachment events occurred. H<sub>2</sub> production with NHM5 dropped to 150 μmol H<sub>2</sub> l<sup>-1</sup> h<sup>-1</sup>. For AMC 414, a slight increase in H<sub>2</sub> production was observed (up to 100 μmol H<sub>2</sub> l<sup>-1</sup> h<sup>-1</sup>). Reestablishing a NaHCO<sub>3</sub> concentration of 10 mM in the medium inflow and increasing the light intensity from 25 to 75 μmol photons m<sup>-2</sup> s<sup>-1</sup> led to enhanced biofilm formation, i.e., the establishment of dark green biofilms covering the whole capillary (Figure 3 (III)). Especially AMC 414 showed an increased H<sub>2</sub> production with up to 150-200 μmol H<sub>2</sub> l<sup>-1</sup> h<sup>-1</sup>, to a comparable

level as obtained with NHM5. After 70 days a reduced H<sub>2</sub> production was measured for both strains and to avoid flush-outs the experiment was stopped. Most likely, the elevated light and CO<sub>2</sub> availability caused an increase in O<sub>2</sub>, and a reduction in cell fitness, leading to a biofilm instability. This is supported by experiments with reduced O<sub>2</sub> concentrations (Figure 4), showing that reduction of O<sub>2</sub> can increase biofilm stability and H<sub>2</sub> production. In total, both investigated uptake hydrogenase-deficient strains produced H<sub>2</sub> under all conditions for 70 days in continuous culture mode with biofilm-mediated biomass retention (Figure 3). In these reaction setups, the maximal H<sub>2</sub> formation rate amounted to 300 µmol H<sub>2</sub> l<sup>-1</sup> h<sup>-1</sup> and an average rate of 250 µmol H<sub>2</sub> l<sup>-1</sup> h<sup>-1</sup> was obtained for both strains under respective optimal conditions. The final biomass density with up to 100 g<sub>cdw</sub> l<sup>-1</sup> is one of the highest biomass concentrations achieved in a photobioreactor so far and the specific H<sub>2</sub> production rates calculated for the last time interval averaged between 2-4 µmol H<sub>2</sub> g<sub>cdw</sub><sup>-1</sup> h<sup>-1</sup>. The biomass concentration in the capillaries is highly dynamic, depending on the cultivation conditions. Thus, specific rates in the earlier stages in the experiments shown in Figure 3, when cell concentrations were lower (in the range between 10 to 100 g<sub>CDW</sub> L<sup>-1</sup>), can be assumed to have been higher. As a consequence, the given specific activity range of 2-4 µmol H<sub>2</sub> g<sub>cdw</sub><sup>-1</sup> h<sup>-1</sup> constitutes a lower boundary.

The possibility to utilize diazotrophic cyanobacteria in CBRs for H<sub>2</sub> production and possible hurdles to be overcome for sustainable photosynthesis-driven H<sub>2</sub> production was investigated. Previously, it has been shown that CBRs can be utilized to cultivate a range of cyanobacteria, including diazotrophic cyanobacteria. Especially *Tolypotrix* sp. PCC 7712 showed high potential to be applied in CBRs (Bozan et al., 2022). However, genetic accessibility, e.g., to knock out uptake hydrogenases, favors other strains like *Nostoc punctiforme* ATCC 29133 NHM5 ( $\Delta hupL$ ) and *Anabaena* sp. PCC

7120 AMC 414 ( $\Delta xisC$ , recombinase). In good accordance with Bozan et al. (2022), the experiments show that biofilm formation with these strains profits from the presence of a heterotrophic biofilm building strain like *P. taiwanensis*. Further, biofilm formation was significantly better in nitrogen free- as compared to normal BG-11 medium.

Furthermore, it was shown that light and elevated carbon availability improved biofilm formation and, associated with it,  $H_2$  production. Several studies demonstrated that both strains produce  $H_2$  in flask and bioreactor experiments under batch cultivation conditions (Lindberg et al., 2002, Lindblad et al., 2002, Masukawa et al., 2002, Avilan et al., 2018). The time range, in which  $H_2$  is produced could be significantly extended to 70 days with improved cultivation conditions. It was possible to produce  $H_2$  continuously over weeks. Previous studies showed short production phases of maximally 30 days (Kosourov et al., 2014; Touloupakis et al., 2016) under batch conditions. Ethylene, also a gaseous product, was recently produced in a similar biofilm-based approach for 38 days (Vajravel et al., 2020). In accordance with the presented results, the authors could also demonstrate that product formation depends on light and carbon availability.

The biomass concentrations reached in the CBRs are among the highest reported for cyanobacteria in bioreactors. Compared to conventional photobioreactors with biomass densities up to  $20 \text{ g}_{\text{cdw}} \text{ l}^{-1}$  (Bähr et al., 2016) and other biofilm photobioreactor designs (up to  $60 \text{ g}_{\text{cdw}} \text{ l}^{-1}$ , Wang et al., 2017), the reported CBR setup enabled the highest biomass concentration ( $100 \text{ g}_{\text{cdw}} \text{ l}^{-1}$ ) reported so far for phototrophic microorganisms. On the other hand, with a different purpose, i.e., production of biomass, value-added products therein, or waste water treatment, only porous substrate-based photobioreactors (PSBRs) showed a higher biomass production up to  $300 \text{ g}_{\text{cdw}} \text{ l}^{-1}$  (Podola et al., 2017). Yet, in PSBRs, biofilms are not in direct contact with

cultivation liquid, and normalizing biomass amounts produced to the cultivation liquid volume is complex, with productivities and economics for biomass harvest rather to be calculated relative to the area as g dry mass per m<sup>2</sup> and day (Li et al., 2019). In addition, efficient applications of PSBRs for extracellular chemical or biofuel products are not reported and seem to be challenging, due to product evaporation, mass transfer, and biofilm ageing. This is especially the case for gaseous products.

### Biofilm formation and H<sub>2</sub> production is light dependent

The experiment shown in Figure 3 indicated a significant influence of the light intensity on H<sub>2</sub> formation and surface coverage of biofilms of cyanobacteria in consortia with Pseudomonads. Thus, the light dependency of H<sub>2</sub> formation by NHM5 and AMC 414 was analyzed further. The CBRs were operated as described above with air segments in a slug flow mode. Cultivation and H<sub>2</sub> formation were tested at five different light intensities (50, 75, 100, 125, and 150  $\mu\text{mol photons m}^{-2} \text{ s}^{-1}$ ) with 10 mM NaHCO<sub>3</sub> in the medium. Each light intensity was applied for five days and the corresponding H<sub>2</sub> formation rates were determined (Figure 4 A+B). For NHM5-based biofilms, volumetric H<sub>2</sub> formation rates increased with the light intensity up to 125  $\mu\text{mol photons m}^{-2} \text{ s}^{-1}$  to a maximum of 75  $\mu\text{mol H}_2 \text{ l}^{-1} \text{ h}^{-1}$ . It is important to note that volumetric production rates were lower compared to the long-term experiments, since final biomass concentrations were lower (between 30-50 g<sub>CDW</sub> l<sup>-1</sup>). A further increase in light intensity led to reduced H<sub>2</sub> formation accompanied by increasing O<sub>2</sub> concentrations. At high light intensities, cells and biofilm fragments detached from the capillaries, were flushed out, and consequently H<sub>2</sub> production stopped (data not shown). It is important to note that biofilms recovered in a few days inside the capillaries after the light intensity was reduced again to 50  $\mu\text{mol photons m}^{-2} \text{ s}^{-1}$ . Also, AMC 414 biofilms showed increased H<sub>2</sub> production with increasing light intensity. Production rates increased from 35 to 75

$\mu\text{mol H}_2 \text{ l}^{-1} \text{ h}^{-1}$  at  $150 \mu\text{mol photons m}^{-2} \text{ s}^{-1}$ . At high light intensity, biofilm detachment was observed as for NHM5. Previously, David et al., 2015 estimated light attenuation within a cyanobacterial biofilm. Theoretically, for a light intensity of  $150 \mu\text{mol photons m}^{-2} \text{ s}^{-1}$  and a light attenuation coefficient of  $9 \text{ mm}^{-1}$ , a maximal biofilm thickness of  $250 \mu\text{m}$  can be achieved. It is not clear, how far light can penetrate into biofilm. In natural microbial mats, cyanobacterial layers can reach several mm. This indicates, that there is enough light available also in deeper layers. Furthermore, there are reports on *Synechocystis*, which hypothesize cells acting as a kind of micro-lens, transporting light from one end of the cell to the other and thereby guide it to deeper levels of biofilms (Schuergers et al 2016). In our experiments, light was supplied only from the top, but the capillary surface was covered completely (also the bottom part) indicating, that in this range enough light is available to allow complete surface coverage of the capillary.

Besides  $\text{H}_2$ ,  $\text{O}_2$  was monitored, as elevated  $\text{O}_2$  concentrations are known to impair cell vitality and nitrogenase activity (Zhao et al., 2007). Air segments contained 20.9%  $\text{O}_2$  at the inflow. During cultivation at low light intensities,  $\text{O}_2$  concentrations were constant between 18-20% after 10 min of residence time, whereas high light intensities led to  $\text{O}_2$  levels up to 23.5% in the gas phase. It is important to note that gas diffusion through the tubes cannot be excluded. The high light in combination with elevated  $\text{O}_2$  concentrations and the risk of ROS formation might contribute to the destabilization and final detachment of the biofilm at higher light intensities.

To further elucidate the correlation of elevated  $\text{O}_2$  concentrations and biofilm detachment,  $\text{N}_2$  and Argon instead of air have been applied to the CBRs in segmented flow mode at a constant illumination of  $100 \mu\text{mol photons m}^{-2} \text{ s}^{-1}$  (Figure 4 C+D). The overall  $\text{O}_2$  concentration in the CBR was thus lowered and only 15 – 20 % of  $\text{O}_2$  was

measured in the gas phase at the outlet of the different set-ups. It is important to note that no completely anaerobic and N<sub>2</sub>-depleted conditions were established as the medium feed was air-saturated and gas diffusion through the tubes cannot be excluded. The changed gas stream stabilized the biofilms in the CBRs and no biofilm detachments were observed, indicating that increased O<sub>2</sub> concentrations at elevated light intensities promoted biofilm detachment. In the case of AMC 414, H<sub>2</sub> production rates slightly decreased upon replacement of air with N<sub>2</sub> or argon. However, NHM5 showed a 50% increase in H<sub>2</sub> production when supplied with argon. It is important to note that argon was expected to increase H<sub>2</sub> formation, as this has been found before in short term experiments (Wilson et al., 2021), but would result in a limited N<sub>2</sub> fixation. Here, a sufficient N<sub>2</sub> supply was assured via the medium feed. GC measurements showed a decrease to 40% at the outflow, instead of 80% N<sub>2</sub> in air.

The results demonstrated that light and CO<sub>2</sub> availability are main factors determining H<sub>2</sub> production rates in diazotrophic cyanobacteria, since H<sub>2</sub> production is directly linked to growth in these cells. Also, other nutrients influence H<sub>2</sub> production, but their direct effects on H<sub>2</sub> production are still unclear (Howe et al., 2020; Lindberg et al., 2004).

Another important factor in CBRs is the gas supply. Under slug flow conditions based on air segments, the O<sub>2</sub> concentrations in CBRs are typically close to that in air or slightly above. However, high photosynthetic rates induced by high light and elevated CO<sub>2</sub> availabilities are accompanied by elevated O<sub>2</sub> production. As a result of the light stress accompanied by high O<sub>2</sub> levels and most likely ROS (reactive oxygen species) formation biofilm stability is affected. Several studies showed similar results (Heuschkel et al., 2020; Hoschek et al., 2019). Elevated O<sub>2</sub> concentrations can promote ROS production, which may result in biofilm detachment (Heuschkel et al., 2020). For effective bioprocessing with phototrophs in biofilms, measures are needed



to remove O<sub>2</sub> efficiently, either by utilizing oxygen free gas segments or by means of oxygen consuming heterotrophic cells (Heuschkel et al., 2020). Since the focus of the study was set to determine photosynthesis-driven H<sub>2</sub> production, any organic carbon source for heterotrophs was omitted. Exchange of the air segments with N<sub>2</sub> or Argon reduced O<sub>2</sub> concentrations in the biofilms/capillaries (below 20%) and stabilized H<sub>2</sub> production or even lead to a 50% increase in hydrogen production as shown for NHM5. The capillary photobioreactor in combination with segmented flow, allows long-term H<sub>2</sub> production and opens the door towards product removal since gaseous H<sub>2</sub> can be extracted from the reaction environment via the air segments, considering appropriate measures to avoid diffusional losses of this highly diffusive gas.

In this study, it was shown that light and CO<sub>2</sub> are limiting factors regarding H<sub>2</sub> production (Figure 4), as increased light intensity increases H<sub>2</sub> production. However, the upper limits for PBRs in terms of light intensity have to be determined in the future.

Recent studies determined additional factors influencing H<sub>2</sub> production, e.g. biofilm thickness, and methods were reported, e.g. fiber optics, to measure and manipulate thickness (Zhong et al., 2014). In our study the biofilm thickness was controlled by the segmented flow, allowing the development of a stable and dense biofilms, see also (Bozan et al., 2022). Finally, new sensors and methods to manipulate light penetration, to measure H<sub>2</sub> production online in biofilms (Chen et al., 2019; Guo et al., 2011; Li et al., 2017) are designed and could help to determine heterogeneities in biofilms regarding H<sub>2</sub> production and this knowledge can help to improve biofilm development and finally H<sub>2</sub> production.

Comparison with H<sub>2</sub> formation rates reported in literature showed that rates determined in this study under continuous biofilm cultivation conditions are lower (~3 μmol H<sub>2</sub> g<sub>cdw</sub><sup>-1</sup> h<sup>-1</sup>, but varying with applied biofilm density) than in suspended batch

cultures ( $\sim 15 \mu\text{mol H}_2 \text{ g}_{\text{cdw}}^{-1} \text{ h}^{-1}$ ) and compared to literature ( $50\text{-}100 \mu\text{mol H}_2 \text{ g}_{\text{cdw}}^{-1} \text{ h}^{-1}$ ). Yet, such batch cultures show a high nitrogenase activity only during the exponential growth phase (Lichtl et al., 1997). However, the biofilm co-cultures showed activity for  $\text{H}_2$  formation for several weeks. It has to be pointed out, that one has to differentiate between low and high biofilm densities, the first show a higher activity and the second lower rates, pointing towards more maintenance activity in high-density biofilms and low growth. Likewise, novel and advanced methods will help to determine growth rates in combination with  $\text{H}_2$  production rates in a temporally and spatially resolved way (Chen et al., 2019; Guo et al., 2011; Li et al., 2017). Additionally, it is challenging to compare  $\text{H}_2$  formation rates directly since rates calculated from short-term assays do not always reflect actual product formation rates achievable in the longer term. Importantly, one has to consider  $\text{H}_2$  loss by diffusion through the capillaries, as indicated by the experiments with argon and nitrogen.

The continuous  $\text{H}_2$  production for weeks in the capillary photobioreactors with both cyanobacterial strains indicates that nitrogenases are active in diazotrophs and cyanobacteria cells retain their activity over a long time. However, the activity in high cell density biofilms was lower, pointing towards low growth and probably maintenance activity. Diazotrophic cyanobacteria can be utilized to provide a stable anaerobic environment inside a heterocyst cell. Such strains are ideal models for developing technical processes for photosynthesis-driven  $\text{H}_2$  production. Furthermore, carbon and nitrogen fixation can be combined with the process of  $\text{H}_2$  production thus avoiding additional nitrogen sources in cultivation media. Finally, a (dynamic) heterogeneity of the ratios of different microbial species in catalytic biofilms might be of importance for the productivity of  $\text{H}_2$  production and will be subject to future studies.

418

## 419 Suitability of CBRs in the industrial use for H<sub>2</sub> production

420 Capillary units are used as standard tools in continuous industrial processes for the  
421 separation or production of matter up to scales of many thousands of tons or m<sup>3</sup> per  
422 year. One principle of increasing product volumes (scaling) of these microreactors is  
423 the numbering up of individual reactor units (Dong et al., 2021). Assuming a theoretical  
424 numbering up of the reaction units used in the CBR setup based on a monolayer of  
425 capillaries next to each other on a total flat area of 100 m \* 100 m (1 ha) without  
426 considering the actual design or geometry of the final unit: Scale-up of the biofilm  
427 photobioreactor (CBR) to 100 m<sup>2</sup> would in theory yield about 10 kg dry biomass,  
428 considering a flat single-layer setup with about 13200 reaction units of the CBR setup  
429 (25 cm length, 3 mm outer diameter, 1 ml volume). In the present study, mature biofilms  
430 with 100 g<sub>cdw</sub> l<sup>-1</sup> produced on average 3 μmol H<sub>2</sub> g<sub>cdw</sub><sup>-1</sup> h<sup>-1</sup>. Considering 1000 h sunshine  
431 a<sup>-1</sup> as a rough average estimation for Germany, this would correspond to 6 kg H<sub>2</sub> to be  
432 produced in an area of 1 hectare in one year. Assuming the same basic reaction setup  
433 with a different biocatalyst for H<sub>2</sub> production based on a hydrogenase with a turnover  
434 number of 100 s<sup>-1</sup> instead of the nitrogenase (1 s<sup>-1</sup>) for H<sub>2</sub> formation might already  
435 reach an impressive range for small-scale technical applications. Furthermore, three-  
436 dimensional constructions instead of monolayer designs, e.g., artificial, leaf-like, or  
437 vertical structures, can be expected to significantly enhance the productivity per area.

438 Together with the specific biocatalyst activity, several other factors are critical for  
439 efficient biotechnological applications, i.e., light penetration, achieved cell densities,  
440 energy costs for mixing and cooling, and efficient product recovery. The approach  
441 presented here, showed that capillary photobioreactors enable continuous production  
442 formats and very high cell densities. Reduction of the O<sub>2</sub> concentration was essential

to ensure biofilm stability. Utilizing artificial gas mixtures reduced O<sub>2</sub> under what can be considered as a critical level. Thus, controlling gas concentrations is crucial for technical applications. Argon atmosphere increases H<sub>2</sub> production by a factor of 4 compared to N<sub>2</sub> fixing conditions (Lindblad et al., 2002). This, however, is not feasible in the long term, since nitrogen fixation is essential for cell survival. In conclusion, beneficial effects regarding biofilm formation and H<sub>2</sub> production could be obtained by manipulating the gas composition of the air segments. In combination with an optimal light and carbon provision, an improved and stable H<sub>2</sub> production in CBRs was achieved in continuous mode over weeks with high biomass concentrations. Other critical factors to be addressed in the future include medium demands, temperature effects, and gas diffusion through capillary materials. Overall, designing catalysts with high activity and realizing scalability are now the major challenges to be addressed.

## Conclusion

The results demonstrated the principal feasibility of CBRs to produce gaseous products like H<sub>2</sub>. This opens the door for future application, especially H<sub>2</sub> production based on hydrogenases in phototrophic organisms. CBRs can now be utilized to investigate essential parameters regulating biofilm development, structure, stability, and scale-up efficiencies. However, several factors still limit technical application, especially medium recycling and methods for gas separation. As the final production process will occur under natural conditions, also the effects of day/night cycles, temperature variations, etc., have to be investigated. Nevertheless, CBRs allow the photosynthesis driven production of a gaseous product in a continuous mode, with a highly active biomass.

E-supplementary data for this work can be found in e-version of this paper online.

## Acknowledgement

We are grateful for discussions with Jens Appel inspiring our work on uptake hydrogenase deficient strains of *Anabena* sp. and *Nostoc* sp.. We thank Pia Lindberg for providing the strains. We acknowledge the use of the facilities of the Centre for Biocatalysis (MiKat) at the Helmholtz Centre for Environmental Research, which is supported by European Regional Development Funds (EFRE, Europe funds Saxony). Rohan Karande was funded by the Federal Ministry for Economic Affairs and Energy (BMW, STARK program, project number 46SKD023X) and is co-financed by the Saxon state parliament (SMWK).

## References

1. Avilan, L., Roumezi, B., Risoul, V., Bernard, C.S., Kpebe, A., Belhadjassine, M., Rousset, M., Brugna, M., Latifi, A. 2018. Phototrophic hydrogen production from a clostridial [FeFe] hydrogenase expressed in the heterocysts of the cyanobacterium *Nostoc* PCC 7120. *Appl Microbiol Biotechnol*, **102**(13), 5775-5783.
2. Bähr, L., Wüstenberg, A., Ehwald, R. 2016. Two-tier vessel for photoautotrophic high-density cultures. *J Appl Phycol*, **28**(2), 783-793.
3. Bothe, H. 2016. The potential use of cyanobacteria for the conversion of solar light to molecular hydrogen as a new energy source. *New Biotechnology*, **33**, S51-S52.

4. Bozan, M., Schmid, A., Bühler, K. 2022a. Evaluation of self-sustaining cyanobacterial biofilms for technical applications. *Biofilm*, **4**, 100073.
5. Bühler, K., Bühler, B., Klähn, S., Krömer, J.O., Dusny, C., Schmid, A. 2021. Biocatalytic production of white hydrogen from water using cyanobacteria. in: *Photosynthesis: Biotechnological Applications with Microalgae*, (Ed.) R. Matthias, De Gruyter, pp. 279-306.
6. Chen, M., Xin, X., Liu, H., Wu, Y., Zhong, N., Chang, H. 2019. Monitoring biohydrogen production and metabolic heat in biofilms by fiber bragg grating sensors. *Analytical Chemistry*, **91**(12), 7842-7849.
7. Cheng, D., Ngo, H.H., Guo, W., Chang, S.W., Nguyen, D.D., Bui, X.T., Wei, W., Ni, B., Varjani, S., Hoang, N.B. 2022. Enhanced photo-fermentative biohydrogen production from biowastes: An overview. *Bioresource Technology*, **357**, 127341.
8. David, C., Bühler, K., Schmid, A. 2015. Stabilization of single species *Synechocystis* biofilms by cultivation under segmented flow. *Journal of Industrial Microbiology and Biotechnology*, **42**(7), 1083-1089.

9. Dong, Z., Wen, Z., Zhao, F., Kuhn, S., Noël, T. 2021. Scale-up of micro- and milli-reactors: An overview of strategies, design principles and applications. *Chemical Engineering Science: X*, **10**, 100097.
10. Fernandes, B.D., Mota, A., Teixeira, J.A., Vicente, A.A. 2015. Continuous cultivation of photosynthetic microorganisms: Approaches, applications and future trends. *Biotechnol Adv*, **33**(6 Pt 2), 1228-45.
11. Fu, J., Huang, Y., Liao, Q., Xia, A., Fu, Q., Zhu, X. 2019. Photo-bioreactor design for microalgae: A review from the aspect of CO<sub>2</sub> transfer and conversion. *Bioresour Technol*, **292**, 121947.
12. Guo, C.-L., Zhu, X., Liao, Q., Wang, Y.-Z., Chen, R., Lee, D.-J. 2011. Enhancement of photo-hydrogen production in a biofilm photobioreactor using optical fiber with additional rough surface. *Bioresource Technology*, **102**(18), 8507-8513.
13. Hariskos, I., Posten, C. 2014. Biorefinery of microalgae - opportunities and constraints for different production scenarios. *Biotechnol J*, **9**(6), 739-52.
14. Heuschkel, I., Dagini, R., Karande, R., Bühler, K. 2020. The impact of glass material on growth and biocatalytic performance of mixed-species biofilms in

536 capillary reactors for continuous cyclohexanol production. *Front Bioeng*  
537 *Biotechnol*, **8**, 588729.

538

539 15.Heuschkel, I., Hoschek, A., Schmid, A., Bühler, B., Karande, R., Bühler, K.  
540 2019b. Mixed-trophies biofilm cultivation in capillary reactors. *MethodsX*, **6**,  
541 1822-1831.

542

543 16.Homburg, S.V., Kruse, O., Patel, A.V. 2019. Growth and photosynthetic  
544 activity of *Chlamydomonas reinhardtii* entrapped in lens-shaped silica  
545 hydrogels. *J Biotechnol*, **302**, 58-66.

546

547 17.Hoschek, A., Heuschkel, I., Schmid, A., Bühler, B., Karande, R., Bühler, K.  
548 2019. Mixed-species biofilms for high-cell-density application of *Synechocystis*  
549 sp. PCC 6803 in capillary reactors for continuous cyclohexane oxidation to  
550 cyclohexanol. *Bioresour Technol*, **282**, 171-178.

551

552 18.Howe, C., Becker, D., Steinweg, C., Posten, C., Stensjö, K. 2020. Iron  
553 limitation – A perspective on a growth-restricted cultivation strategy for a H<sub>2</sub>  
554 production system using the diazotrophic cyanobacterium *Nostoc* PCC 7120  
555  $\Delta$ hupW. *Bioresour Technol Rep*, **11**, 100508.

556

557



19. Johnson, T.J., Katuwal, S., Anderson, G.A., Gu, L., Zhou, R., Gibbons, W.R.  
2018. Photobioreactor cultivation strategies for microalgae and cyanobacteria.  
*Biotechnol Prog*, **34**(4), 811-827.
20. Karande, R., Debor, L., Salamanca, D., Bogdahn, F., Engesser, K.H., Bühler,  
K., Schmid, A. 2016. Continuous cyclohexane oxidation to cyclohexanol using  
a novel cytochrome P450 monooxygenase from *Acidovorax* sp. CHX100 in  
recombinant *P. taiwanensis* VLB120 biofilms. *Biotechnol Bioeng*, **113**(1), 52-  
61.
21. Khetkorn, W., Rastogi, R.P., Incharoensakdi, A., Lindblad, P., Madamwar, D.,  
Pandey, A., Larroche, C. 2017. Microalgal hydrogen production - A review.  
*Bioresour Technol*, **243**, 1194-1206.
22. Kirnev, P.C.S., Carvalho, J.C., Vandenberghe, L.P.S., Karp, S.G., Soccol,  
C.R. 2020. Technological mapping and trends in photobioreactors for the  
production of microalgae. *World J Microbiol Biotechnol*, **36**(3), 42.
23. Kosourov, S., Leino, H., Murukesan, G., Lynch, F., Sivonen, K., Tsygankov,  
A.A., Aro, E.M., Allahverdiyeva, Y. 2014. Hydrogen photoproduction by  
immobilized N<sub>2</sub>-fixing cyanobacteria: understanding the role of the uptake

hydrogenase in the long-term process. *Appl Environ Microbiol*, **80**(18), 5807-17.

24. Krishnan, A., Qian, X., Ananyev, G., Lun, D.S., Dismukes, G.C. 2018. Rewiring of cyanobacterial metabolism for hydrogen production: Synthetic biology approaches and challenges. in: *Synthetic Biology of Cyanobacteria*, (Eds.) W. Zhang, X. Song, Springer Singapore. Singapore, pp. 171-213.

25. Li, T., Podola, B., Schultze, L.K.P., Melkonian, M. 2019. Design scenario analysis for porous substrate photobioreactor assemblies. *J Appl Phycol*, **31**(3), 1623-1636.

26. Li, Y., Zhong, N., Liao, Q., Fu, Q., Huang, Y., Zhu, X., Li, Q. 2017. A biomaterial doped with LaB6 nanoparticles as photothermal media for enhancing biofilm growth and hydrogen production in photosynthetic bacteria. *International Journal of Hydrogen Energy*, **42**(9), 5793-5803.

27. Liao, Q., Zhong, N., Zhu, X., Huang, Y., Chen, R. 2015. Enhancement of hydrogen production by optimization of biofilm growth in a photobioreactor. *International Journal of Hydrogen Energy*, **40**(14), 4741-4751.

28. Lichtl, R.R., Bazin, M.J., Hall, D.O. 1997. The biotechnology of hydrogen production by *Nostoc flagelliforme* grown under chemostat conditions. *Appl Microb Biotech*, **47**(6), 701-707.
29. Lindberg, P., Lindblad, P., Cournac, L. 2004. Gas exchange in the filamentous cyanobacterium *Nostoc punctiforme* strain ATCC 29133 and its hydrogenase-deficient mutant strain NHM5. *Appl Environ Microbiol*, **70**(4), 2137-45.
30. Lindberg, P., Schutz, K., Happe, T., Lindblad, P. 2002. A hydrogen-producing, hydrogenase-free mutant strain of *Nostoc punctiforme* ATCC 29133. *Int J Hydrog Energy*, **27**(11-12), 1291-1296.
31. Lindblad, P., Christensson, K., Lindberg, P., Fedorov, A., Pinto, F., Tsygankov, A. 2002. Photoproduction of H<sub>2</sub> by wildtype *Anabaena* sp. PCC 7120 and a hydrogen uptake deficient mutant: from laboratory experiments to outdoor culture. *Int J Hydrog Energy*, **27**(11-12), 1271-1281.
32. Martin, B.A., Frymier, P.D. 2017. A review of hydrogen production by photosynthetic organisms using whole-cell and cell-free systems. *Appl Biochem Biotechnol*, **183**(2), 503-519.
33. Masukawa, H., Mochimaru, M., Sakurai, H. 2002. Disruption of the uptake hydrogenase gene, but not of the bidirectional hydrogenase gene, leads to

enhanced photobiological hydrogen production by the nitrogen-fixing  
cyanobacterium *Anabaena* sp. PCC 7120. *Appl Microbiol Biotechnol*, **58**(5),  
618-24.

34. Nyberg, M., Heidorn, T., Lindblad, P. 2015. Hydrogen production by the  
engineered cyanobacterial strain *Nostoc* PCC 7120  $\Delta$ hupW examined in a flat  
panel photobioreactor system. *J Biotechnol*, **215**, 35-43.

35. Pathak, J., Rajneesh, Maurya, P.K., Singh, S.P., Häder, D.-P., Sinha, R.P.  
2018. Cyanobacterial farming for environment friendly sustainable agriculture  
practices: Innovations and perspectives. *Front Environ Sci*, **6**.

36. Podola, B., Li, T., Melkonian, M. 2017. Porous substrate bioreactors: A  
paradigm shift in microalgal biotechnology? *Trends Biotechnol*, **35**(2), 121-  
132.

37. Posten, C. 2009. Design principles of photo-bioreactors for cultivation of  
microalgae. *Engineering in Life Sciences*, **9**(3), 165-177.

38. Renaudie, M., Dumas, C., Vuilleumier, S., Ernst, B. 2021. Biohydrogen  
production in a continuous liquid/gas hollow fiber membrane bioreactor:  
Efficient retention of hydrogen producing bacteria via granule and biofilm  
formation. *Bioresource Technology*, **319**, 124203.

39. Schuergers, N., Lenn, T., Kampmann, R., Meissner, M.V., Esteves, T.,  
Temerinac-Ott, M., Korvink, J.G., Lowe, A.R., Mullineaux, C.W., Wilde, A.  
2016. Cyanobacteria use micro-optics to sense light direction. *eLife*, **5**,  
e12620.
40. Schultze, L.K.P., Simon, M.-V., Li, T., Langenbach, D., Podola, B., Melkonian,  
M. 2015. High light and carbon dioxide optimize surface productivity in a Twin-  
Layer biofilm photobioreactor. *Algal Research*, **8**, 37-44.
41. Tiwari, A., Pandey, A. 2012. Cyanobacterial hydrogen production - A step  
towards clean environment. *Int J Hydrog Energy*, **37**(1), 139-150.
42. Touloupakis, E., Rontogiannis, G., Benavides, A.M.S., Cicchi, B., Ghanotakis,  
D.F., Torzillo, G. 2016. Hydrogen production by immobilized *Synechocystis* sp  
PCC 6803. *Int J Hydrog Energy*, **41**(34), 15181-15186.
43. Vajravel, S., Sirin, S., Kosourov, S., Allahverdiyeva, Y. 2020. Towards  
sustainable ethylene production with cyanobacterial artificial biofilms. *Green  
Chemistry*, **22**(19), 6404-6414.

671

672 44. Vorndran, E., Lindberg, P. 2016. *In situ*-immobilization of two model

673 cyanobacterial strains in ceramic structures: A new biohybrid material for

674 photobioreactor applications. *J Biotechnol*, **223**, 1-5.

675

676 45. Wang, J.F., Liu, W., Liu, T.Z. 2017. Biofilm based attached cultivation

677 technology for microalgal biorefineries-A review. *Bioresour Technol*, **244**,

678 1245-1253.

679

680 46. Wilson, S.T., Caffin, M., White, A.E., Karl, D.M. 2021. Evaluation of argon-

681 induced hydrogen production as a method to measure nitrogen fixation by

682 cyanobacteria. *J Phycol*, **57**(3), 863-873.

683

684

685 47. Zavrel, T., Faizi, M., Loureiro, C., Poschmann, G., Stuhler, K., Sinetova, M.,

686 Zorina, A., Steuer, R., Cervený, J. 2019. Quantitative insights into the

687 cyanobacterial cell economy. *Elife*, **8**.

688

689 48. Zhang, H., Chen, G., Zhang, Q., Lee, D.J., Zhang, Z., Li, Y., Li, P., Hu, J., Yan,

690 B. 2017. Photosynthetic hydrogen production by alginate immobilized bacterial

691 consortium. *Bioresour Technol*, **236**, 44-48.

692

49. Zhao, W., Guo, Q., Zhao, J. 2007. A membrane-associated Mn-superoxide dismutase protects the photosynthetic apparatus and nitrogenase from oxidative damage in the cyanobacterium *Anabaena* sp. PCC 7120. *Plant and Cell Physiology*, **48**(4), 563-572.
50. Zhong, N., Liao, Q., Zhu, X., Chen, R. 2014. A fiber-optic sensor for accurately monitoring biofilm growth in a hydrogen production photobioreactor. *Analytical Chemistry*, **86**(8), 3994-4001.

702 **Table 1:** Microbial strains used in this study

| Strain                                             | Characteristics                                                              |                          |
|----------------------------------------------------|------------------------------------------------------------------------------|--------------------------|
| <i>Nostoc punctiforme</i><br>ATCC 29133            | Nitrogen fixing filamentous<br>cyanobacterium                                | (Lindberg et al., 2002)  |
| <i>Nostoc punctiforme</i><br>ATCC 29133 NHM5       | Uptake hydrogenase<br>knockout of ATCC 29133<br>( $\Delta hupL$ )            | (Lindberg et al., 2002)  |
| <i>Anabaena</i> sp. PCC 7120                       | Nitrogen fixing filamentous<br>cyanobacterium                                | (Lindblad et al., 2002b) |
| <i>Anabaena</i> sp. PCC 7120<br>AMC 414            | Uptake hydrogenase<br>knockout of PCC 7120<br>( $\Delta xisC$ , recombinase) | (Lindblad et al., 2002b) |
| <i>Pseudomonas</i><br><i>taiwanensis</i><br>VLB120 | Biofilm forming strain                                                       | (Karande et al., 2016)   |

703

704



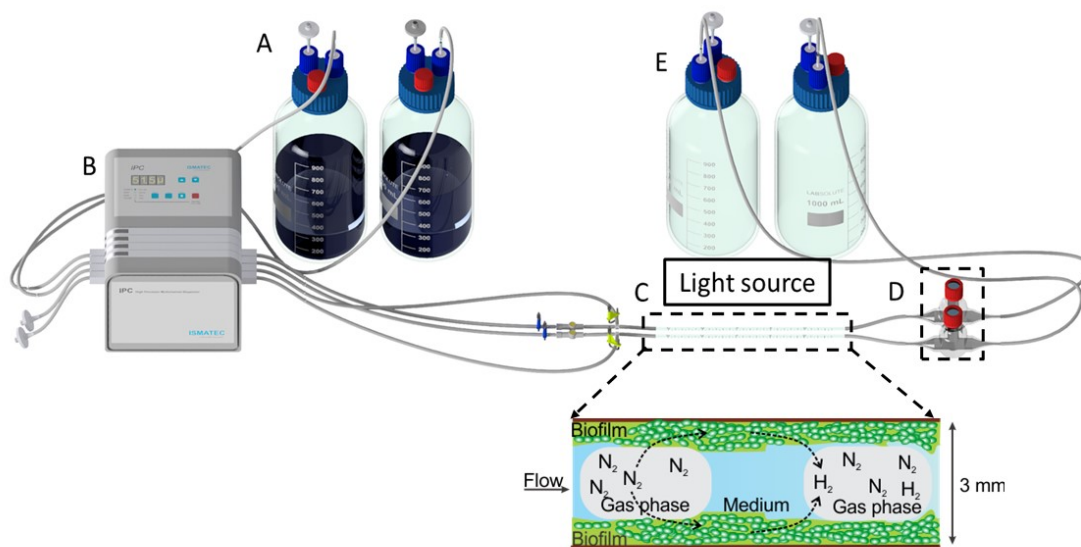
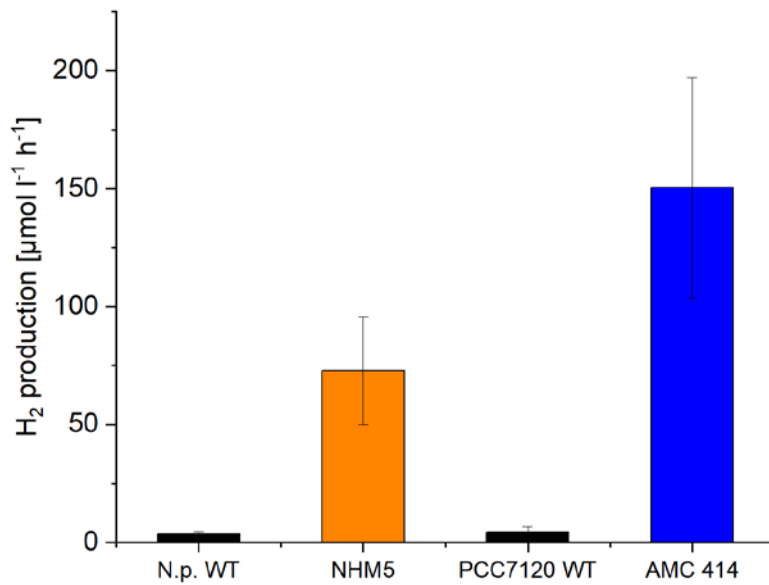


**Figure 1.** Setup of the capillary biofilm reactor system. Figure modified from Heuschkel et al. (2019b), see also for details. (A) Medium bottles, (B) multichannel peristaltic pump, (C) cultivation unit, (D) bubble trap, (E) waste reservoir. The insert depicts a biofilm capillary operated in segmented flow.

718



719

720

721

722

723

724 **Figure 2:** Specific H<sub>2</sub> formation rates of uptake hydrogenase-deficient *N. punctiforme*  
 725 ATCC 29133 NHM5, *Anabaena* sp. PCC 7120 AMC 414, and respective wildtype  
 726 strains in capillary photobioreactors. Plotted are the average H<sub>2</sub> production rates in  
 727 μmol H<sub>2</sub> l<sup>-1</sup>h<sup>-1</sup> as measured daily for 14 days in biological duplicates. Biofilms were  
 728 cultivated as mixed species cultures (with *P. taiwanensis* VLB 120) in 1 ml capillaries  
 729 under continuous illumination (25 μmol photons m<sup>-2</sup> s<sup>-1</sup>) under constant BG-11<sub>0</sub>  
 730 medium and air flow rates of 52 μl min<sup>-1</sup>, each.

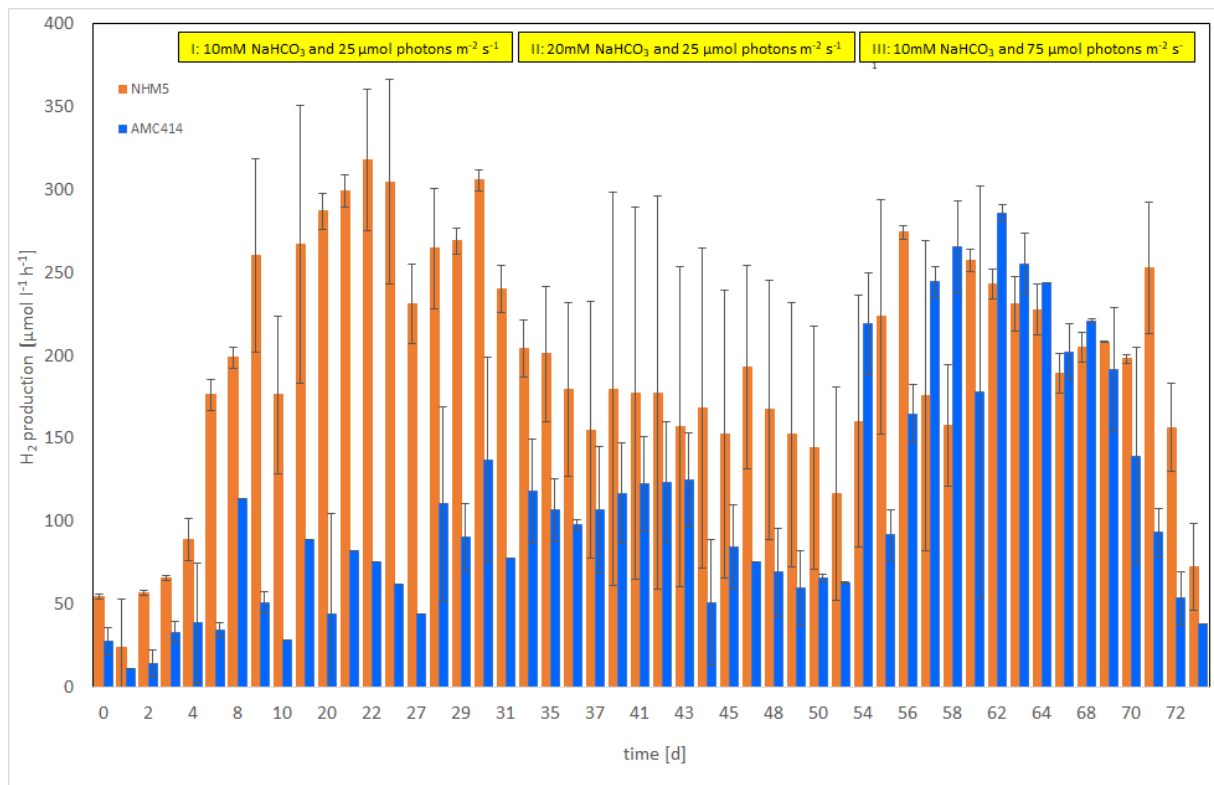


**Figure 3:** Specific H<sub>2</sub> formation rates of *N. punctiforme* ATCC 29133 NHM5 (orange) and *Anabaena* PCC 7120 AMC 414 (blue) in capillary photobioreactors. Biofilms were cultivated in 1 ml capillaries with 10 mM NaHCO<sub>3</sub> in BG-11<sub>0</sub> medium and 25 μmol photons m<sup>-2</sup> s<sup>-1</sup> (time window I), 20 mM NaHCO<sub>3</sub> and 25 μmol photons m<sup>-2</sup> s<sup>-1</sup> (II), and 10 mM NaHCO<sub>3</sub> and 75 μmol photons m<sup>-2</sup> s<sup>-1</sup> (III) for 75 days under a constant medium / air flow of 52 μl min<sup>-1</sup>. Experiments were performed in duplicates, and H<sub>2</sub> concentrations were measured daily as described in Materials & Methods.

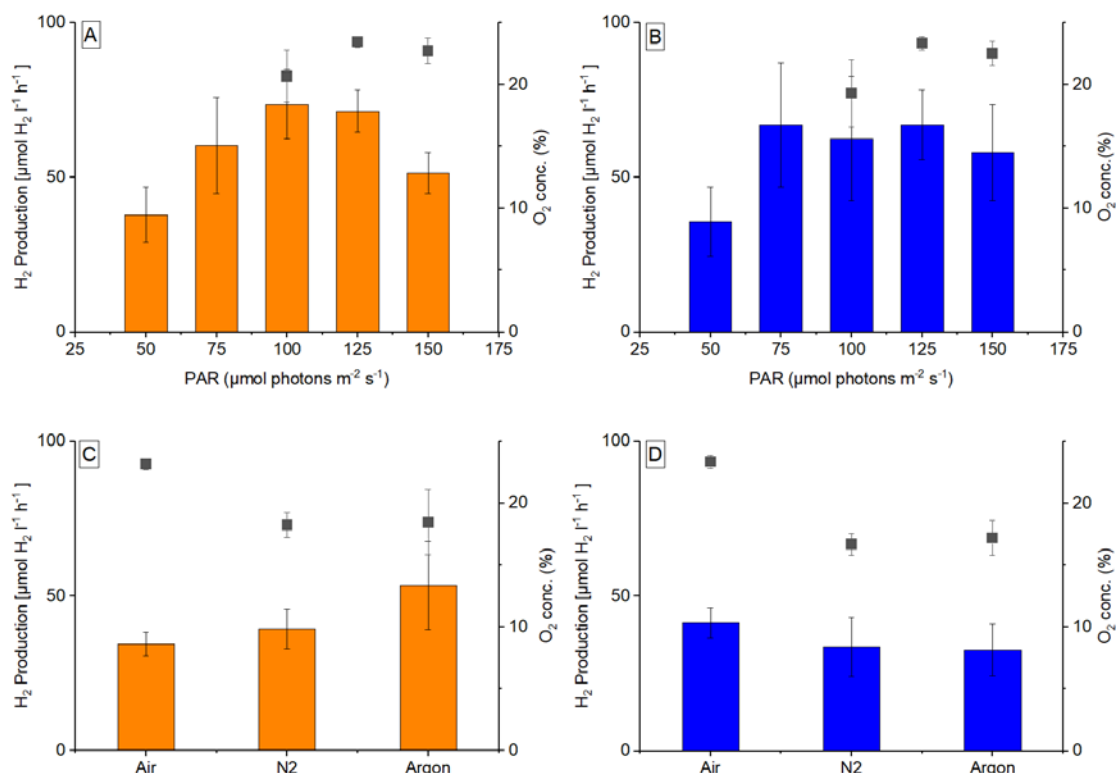


**Figure 4:** H<sub>2</sub> formation of *N. punctiforme* ATCC 29133 NHM5 (A, C, orange) and *Anabaena* PCC 7120 AMC 414 (B, D, blue) in biofilm photobioreactors given as volumetric rates in dependency of the incident light (A, B) and the applied gas phase (C, D). **A+B:** Biofilms were cultivated in 1 ml capillaries at light intensities of 50-150 μmol photons m<sup>-2</sup> s<sup>-1</sup> in BG-11<sub>0</sub> with 10 mM NaHCO<sub>3</sub> under a constant medium and air flow rate of 52 μl min<sup>-1</sup>, each. Light conditions were kept constant for 7 days, and experiments were performed as biological duplicates. H<sub>2</sub> and O<sub>2</sub> formation were determined daily, and production rates are given as mean values determined on 5 consecutive days after an adaptation phase of 2 days. **C+D:** Biofilms were cultivated in 1 ml capillaries under constant illumination of 100 μmol photons m<sup>-2</sup> s<sup>-1</sup> in BG-11<sub>0</sub> medium with 10 mM NaHCO<sub>3</sub>. Different gases were provided via the gas segments (Air, N<sub>2</sub>, and Argon), and conditions were kept constant for 5 days. H<sub>2</sub> and O<sub>2</sub> formation were measured daily. Experiments were performed in biological duplicates and production rates are shown as mean values.